THE JOURNAL OF PHYSICAL CHEMISTRY Letters

pubs.acs.org/JPCL Letter

Exotic Two-Dimensional Structure: The First Case of Hexagonal NaCl

Kseniya A. Tikhomirova, Christian Tantardini, Ekaterina V. Sukhanova, Zakhar I. Popov, Stanislav A. Evlashin,* Mikhail A. Tarkhov, Vladislav L. Zhdanov, Alexander A. Dudin, Artem R. Oganov, Dmitry G. Kvashnin, and Alexander G. Kvashnin*

Cite This: *J. Phys. Chem. Lett.* 2020, 11, 3821−3827 Read Online

ACCESS | Metrics & More | Article Recommendations | Supporting Information

ABSTRACT: NaCl is one of the simplest compounds and was thought to be well-understood, and yet, unexpected complexities related to it were uncovered at high pressure and in low-dimensional states. Here, exotic hexagonal NaCl thin films on the (110) diamond surface were crystallized in the experiment following a theoretical prediction based on *ab initio* evolutionary algorithm USPEX. State-of-the-art calculations and experiments showed the existence of a hexagonal NaCl thin film, which is due to the strong chemical interaction of the NaCl film with the diamond substrate.

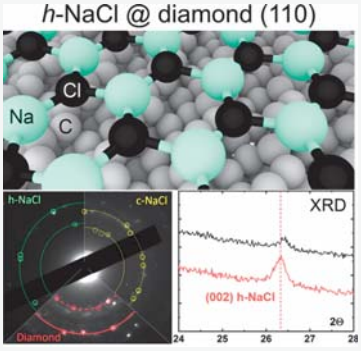

The development of new technologies and devices requires new materials with improved properties. For example, diamond field-effect transistors (FETs) have promising applications for high-power converters in electric vehicle applications and high-power high-frequency amplifiers for telecommunications and radars. Is it desirable to achieve high carrier mobility for these applications, but for diamond FETs it is not possible because of fixed and trapped charges in the nonideal amorphous gate dielectric and the dielectric/diamond interface. The diamond FETs with single crystal hexagonal boron nitride (h-BN) as a gate dielectric have already demonstrated excellent characteristics.[1] We propose that ionic material (i.e., NaCl) with atomic thickness can be used as a gate dielectric in promising diamond FETs because of the wide band gap.[2]

Modern advanced technologies allow scientists to synthesize new two-dimensional (2D) materials of various composition and often with an unexpected crystal structure that has no counterparts in the bulk. Known examples include silicene[3,4] (2D silicon); stanene[5] (monolayer of tin); borophene[6] (monolayer of boron atoms); and 2D layers of CuO,[7] Fe,[8] FeO,[9] CoC,[10] *etc.*

Two-dimensional compounds can be formed between elements that do not form bulk compounds, e.g., copper borides.[11] Currently, there are three main ways to obtain 2D thin films: (i) mechanical exfoliation[12,13] and (ii) atomic layer[14] and (iii) chemical vapor[15,16] depositions. It is noteworthy that mechanical exfoliation works only for layered crystals where the bulk structure consists of weakly bound layers which can be detached and transferred onto the substrate.[12,13] Thus, it cannot be applied to produce silicene because none of the bulk silicon phases have layered structure.[3,4] Indeed, methods (ii) and (iii) allow the synthesis of different 2D structures like silicene and borophene, which are stable only on the substrate.[3,4,6] The strength of interaction between the 2D layer and substrate together with lattice and symmetry mismatches with the substrate may significantly affect the structure and properties of the grown film.[17−19] For example, heteroepitaxial growth of semiconducting structures is possible only at small lattice mismatches between the substrate and desired semiconducting material.[20]

Alkali halides are a well-known type of materials, widely used in several practical applications and fundamental studies.[21,22] The most common among them is sodium chloride, table salt. Bulk phases of NaCl have rocksalt structure type (B1 structure) and (at high pressure) CsCl-type[23] (B2 structure) structure. Crystallographic plane (100) is the most energetically favorable surface in bulk cubic NaCl.[24,25] During the last decades a series of experimental and theoretical studies were performed to investigate the possibility of synthesizing different NaCl thin films on different substrates: Cu(001),[26,27] Cu(110),[28] Cu(111),[29−35] Cu(311),[26] Cu(221),[35,36] Ni(001),[26] Ag(001),[35,37−39] Ag(111),[35,40,41]

Received: March 19, 2020
Accepted: April 23, 2020
Published: April 24, 2020

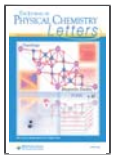

https://dx.doi.org/10.1021/acs.jpclett.0c00874
J. Phys. Chem. Lett. 2020, 11, 3821−3827

Au(111), and Au(111)-(22 × $\sqrt{3}$).[42] The possibility of nonstoichiometric Na_xCl_y thin films was also examined.[43]

Indeed, all performed studies showed the link between the type of substrate and its orientation with the physical and chemical properties associated with NaCl thin film. All these studies infused new lifeblood to the understanding of NaCl thin-film growth showing the possibility of bulk NaCl crystal to form the (111) surface because of more favorable surface reconstructions at specific conditions.[44] This also generated the hypothesis regarding NaCl films of nanometer thickness with unusual hexagonal structure due to documented phase transition from the cubic film with (111) surface to unusual graphitic-like layered film.[45−47] Such surprising findings have led us to expect that the exotic structures of NaCl could be formed and exist on the substrate, which will have a strong binding with it. A combination of the evolutionary algorithm USPEX[48−50] and first-principles calculations are used here to investigate the formation of NaCl films on various substrates: Cu(100); Cu(111); Cu(311); Ag(111); Ag(100); and (100), (110), and (111) diamond surfaces. Predicted structures were synthesized and analyzed with selected area electron diffraction (SAED) and X-ray diffraction.

Different substrates of different compositions, including metallic (Cu and Ag) and diamond surfaces, were considered to simulate the formation of a 2D NaCl structure on them using the evolutionary algorithm USPEX[48−50] capable of predicting the lowest-enthalpy structures knowing just the chemical elements involved. Structure relaxations and energy calculations were done using VASP[51−54] (see Supporting Information for details). The first population of structures for the evolutionary search was randomly produced. All subsequent populations were obtained from the previous population by selection and variation operators. Thus, 40% of the structures were generated by the heredity operator, 10% by soft mutation , 30% transmutation operations, and 20% structures were randomly produced (see Computational Details in the Supporting Information). In the presented calculations, we included all the surface supercells up to index 4 to enable the prediction of complex structures. Each of the considered supercells contained a vacuum layer of 20 Å. Metallic substrate slabs were 5 atomic layers thick (thickness ≈ 6 Å), the uppermost 3 Å of which was allowed to relax. In the case of the diamond, the thickness of substrates was about 8 Å, corresponding to 4−5 atomic carbon layers depending on orientation. We also performed test calculations using slabs with doubled thickness, and only the bottom layer was kept fixed to obtain more accurate surface energies for stable structures. No significant differences were found, which confirms the reliability of our calculations. To simulate the formation of two-dimensional layers on the substrate it is necessary to prevent the penetration of the deposited atoms inside the substrate. Thus, we have modified the algorithm giving the possibility of adding a small vacuum gap between the substrate and the deposited atoms.

The binding energy between the thin film and the substrate is a measure of their interaction and is defined as

$$E_{bind} = E_{tot} - E_{subst} - E_{NaCl} \quad (1)$$

where E_{tot} is total energy of the whole system (film on the substrate); E_{subst} and E_{NaCl} are the energies for isolated substrate and NaCl thin film, respectively. The binding energies between NaCl films and substrates were calculated assuming, in these initial estimates single and double layered cubic (100)-NaCl films placed on each type of substrate as the most stable found in previous works.

As prototypical metal substrates we considered Cu(100), Cu(111), Cu(311), Ag(111), and Ag(100) because they are often used for crystal growth of thin films. In addition to metallic substrates, also diamond surfaces with (100), (110), and (111) crystallographic orientations were considered, because diamond is a prototypical covalent material, the surface behavior of which is expected to differ greatly from that of metals.

As was expected, the binding energy per unit surface area between the 2D NaCl and metal surfaces is very tiny (see Figure 1), which means negligible interaction between them.

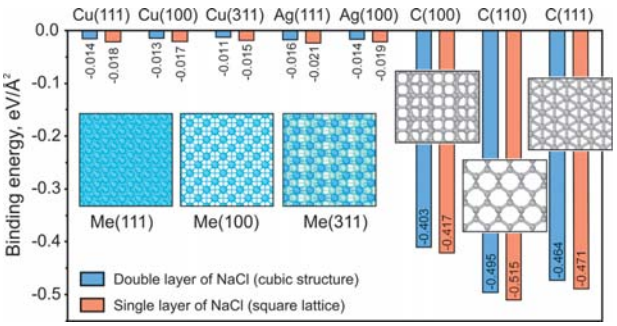

Figure 1. Binding energy per unit surface area between single (orange) and 2-layered (blue) cubic NaCl film with (100) and different substrates, including Cu(111); Cu(100); Cu(311); Ag(111); Ag(100); and diamond with (100), (110), and (111) orientations. The insets show top view of metallic and diamond surfaces of various orientations used for calculations.

Thus, the thin films of NaCl is practically independent of either the type of metal or crystallographic orientation of the substrate. The absolute values of binding energies by order of magnitude correspond to the van der Waals interaction;[55] the exact values varied between −0.011 and −0.017 eV/Å^2.[2] Simulations of NaCl monolayer film on metallic substrates performed with the evolutionary algorithm USPEX showed that it is unstable and tends to form a cluster on the surface (see NaCl Film on Metal Substrates in the Supporting Information), because the weak interaction with the substrate cannot compensate for the loss of three-dimensional binding.

The binding energies evaluated for diamond surfaces are *ca.* 30 times greater than that for metal substrates (Figure 1) and equal to −0.40, −0.49, and −0.46 eV/Å^2 for (100), (111), and (110) surfaces, respectively. Thus, the possibility of making 2D structures is higher in the case of diamond compared to metal substrates because of the low binding energy of the latter with NaCl. Strong binding can also lead to the formation of exotic thin films of NaCl.

The initial hypothesis that there should be a correlation between binding energy and the propensity to form exotic thin films was subsequently investigated by simulations of NaCl ultrathin film on diamond surfaces using the evolutionary algorithm USPEX.

The simulations were performed using layer-by-layer procedure of formation. After the simulation of the first layer, which is optimized to find the thermodynamically stable configuration, the second layer is simulated on top of the previous one and subsequently optimized together with the fist layer. This procedure was repeated several times to achieve 3−

https://dx.doi.org/10.1021/acs.jpclett.0c00874
J. Phys. Chem. Lett. 2020, 11, 3821−3827

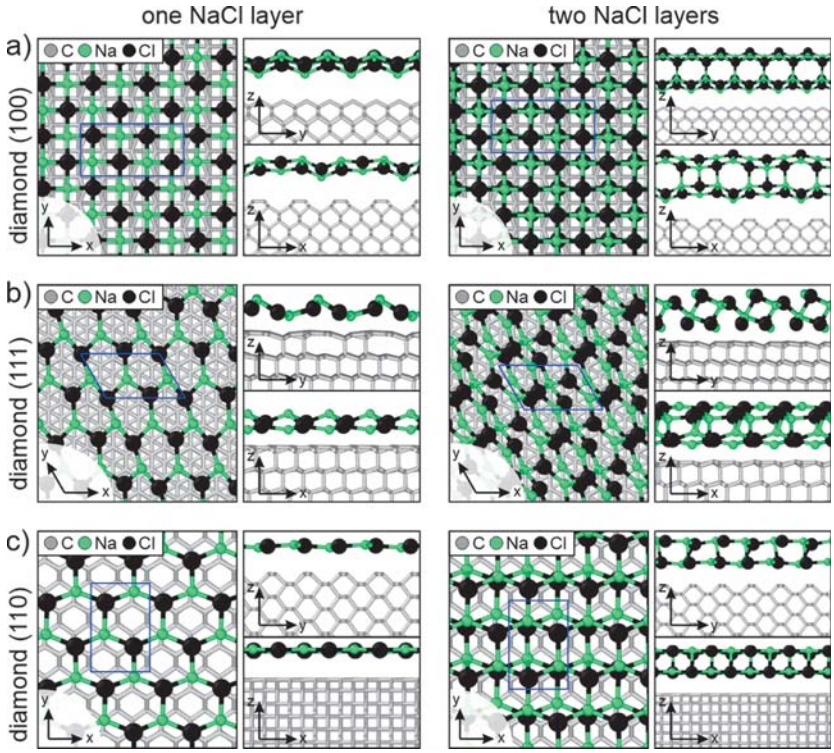

Figure 2. Crystal structure of single- and double-layered NaCl films formed on the diamond substrate with (a) (100), (b) (110), and (c) (111) surfaces. Legend: white spheres, carbon; small green spheres, chlorine; big turquoise spheres, sodium.

4 layers formed on the diamond substrate. The NaCl monolayer formed on the (100) diamond surface is a 2D crystal with a distorted tetragonal structure (Figure 2a). This ultrathin film can be considered as a distorted single layer of (100) surface of cubic NaCl with lattice parameters a = 10.02 Å and b = 5.03 Å. The second simulated NaCl layer has a structure similar to the first one (Figure 2a). Both NaCl layers are aligned with each other, despite corrugation due to large strain: lattice mismatch between the free-standing 2-layered NaCl and diamond (100) surface is 12%. This will lead to the formation of a large number of possible atomic arrangements, which will increase the possibility of obtaining exotic 2D structures.

The simulation of ultrathin film deposition on the (111) diamond surface showed a nonflat first NaCl layer, without any resemblance to other known NaCl structures (Figure 2b). This result is completely different from what we saw for the (100) surface (Figure 2a). Such a distorted structure was also obtained in the simulation of the second layer (Figure 2b). Remarkably, the simulation of an ultrathin NaCl film on the (110) surface of diamond showed the formation of NaCl with a pseudohexagonal honeycomb-like structure with orthorhombic symmetry (Figure 2c). It is noteworthy that the subsequently deposited layers are not corrugated.

The nature of chemical bonding between predicted NaCl films and diamond surfaces was initially investigated using the electron localization function (ELF).[56] The calculated ELF at the isosurface equal to 0.8 (see Figure S6) does not demonstrate electron localization between NaCl and carbon atoms. Thus, we performed an investigation of noncovalent interactions (NCIs) for the fully optimized structures of NaCl on the (100), (110), and (111) diamond surfaces through the calculations of reduced density gradient (RDG, defined as $s = 1/(2(3\pi^2)^{1/3})\cdot\nabla\rho/\rho^{4/3}$).[57−60] The RDG plotted at isosurface s = 0.5 between NaCl thin film and diamond surfaces (Figure 3a,c,e) showed NCIs in the order of vdW interactions through the blue−green−red scale according to values of sign(λ_2)ρ (λ_2 is the second electron density Hessian eigenvalue):[57−60] <−0.02, H-bond (i.e., blue); −0.02 to 0.02, vdW (i.e., green); >0.02, steric repulsion (i.e., red). The presence of vdW interactions is confirmed also by the graphs of s versus sign(λ_2)ρ (Figure 3b,d,f). This function was calculated and drawn for the fully optimized structures using CRITIC2 program.[61,62] Furthermore, considering details of the interaction on the (110) surface, the RDG analysis showed an interaction in the order of a weak H-bond (inset of Figure 3c and red line in Figure 3d) with s at the border between vdW interactions and H-bond (i.e., sign(λ_2)ρ < −0.02). This confirms our previous results about the strongest interaction between NaCl and diamond (110) surface allowing the formation of exotic 2D structure.

The obtained pseudohexagonal structure agrees with the extension of the Curie principle to 2D materials that the symmetry of the formed thin film cannot be higher than the symmetry of the substrate.

We deposited NaCl thin film on the polycrystalline diamond substrate as well as on the single-crystal diamond substrates of (111), (100), and (110) surfaces to confirm the possibility of the formation of predicted exotic (pseudo) 2D h-NaCl. The results of NaCl deposition were analyzed with scanning electron microscopy (SEM), showing the presence of films with cubic structure (see Figure S7). Transmission electron microscopy (TEM) and X-ray diffraction (XRD) are carried out to determine the type of crystal lattice.

https://dx.doi.org/10.1021/acs.jpclett.0c00874
J. Phys. Chem. Lett. 2020, 11, 3821−3827

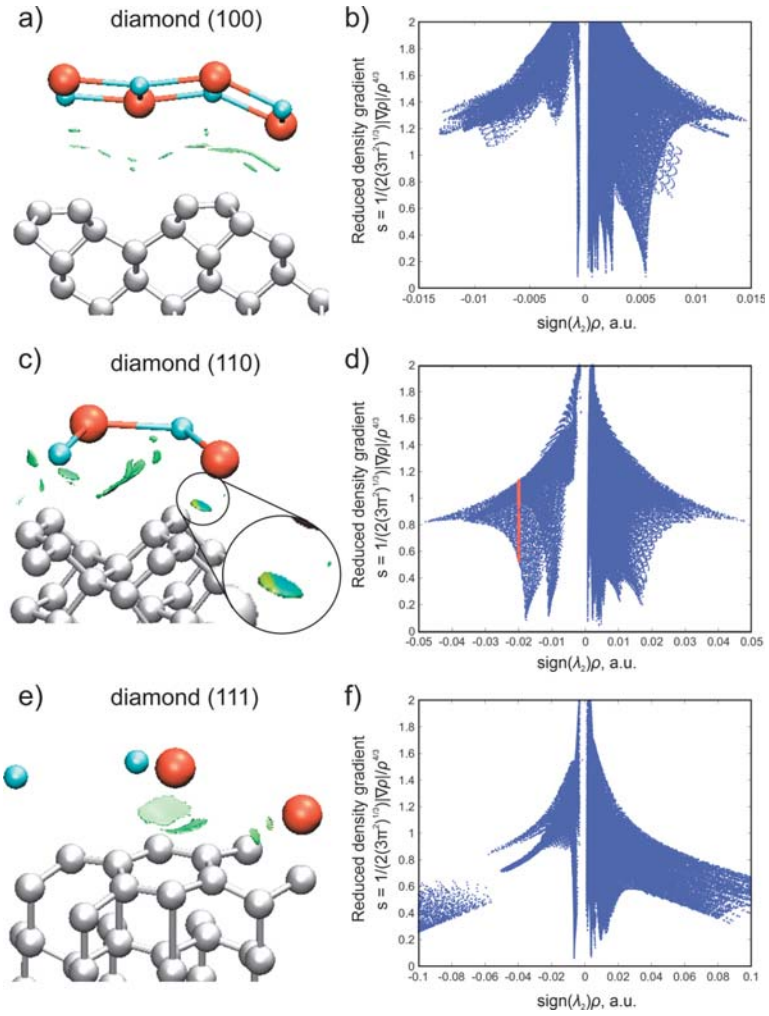

Figure 3. Analysis of noncovalent interactions in studied systems of NaCl films on diamond with (a) (100), (c) (110), and (e) (111) surfaces. Gradient isosurface for $s = 0.5$ and $-0.08 < \mathrm{sign}(\lambda_2)\rho < 0.08$ [color scale: from blue (strong attractive interactions) through green (moderate vdW interactions) to red (strong nonbonded overlap)]. (b), (d), (f) Plots of the reduced density gradient (s) versus the electron density multiplied by the sign of the second Hessian eigenvalue ($\mathrm{sign}(\lambda_2)\rho$). The color scheme is as follows: orange for chloride; turquoise for sodium; and white gray for carbon.

The presence of h-NaCl was initially evaluated on the polycrystalline diamond through SAED from various areas of the sample, and the results were then merged into one image (Figure 4a). SAED images show the presence of the reflections related to several different materials, such as diamond (red in Figure 4a) and cubic NaCl (green in Figure 4a), and a set of reflections that do not fit any known materials (yellow in Figure 4a). We suggest that new reflections belong to the new hexagonal phase of NaCl. Unfortunately, polycrystalline substrates consist of surfaces of all possible crystallographic orientations. Thus, it is not possible to know on which of them the h-NaCl film was grown.

This experiment is consistent with all our theoretical predictions about the formation of NaCl thin films with an exotic hexagonal structure, but it does not provide compelling proof yet. To identify those reflections which do not match known materials in SAED, we performed selected area electron diffraction pattern simulations via LAMMPS software.[63] For technical details, please see Simulation of Selected Area Electron Diffraction Patterns in the Supporting Information. We carried out calculations of SAED patterns for the diamond, c-NaCl, and h-NaCl polycrystals with various grain sizes. In the right panel of Figure 4a, the calculated SAED images are presented. Dashed and solid lines depict the first and second diffraction rings that correspond to the experimentally observed peaks. Calculated diffraction rings (solid lines) were placed on the experimentally obtained signals (circles) to recognize new reflections (Figure 4a). By comparison between experimental and simulated SAED patterns, it is possible to draw conclusions about the existence of h-NaCl after deposition to the diamond (110) surface. All the calculated SAED images are presented in Table S1.

To obtain compelling proof, NaCl was deposited on each of three major diamond surfaces, and the crystal structures of obtained samples were studied with X-ray diffraction (XRD) (see Figure 4b). For detailed information about the XRD technique, please see the section X-ray Scattering in the Supporting Information. The XRD diffraction pattern showed an intense peak for (110) diamond substrate corresponding to (002) reflection of the NaCl hexagonal structure at *ca.* 26.5°

https://dx.doi.org/10.1021/acs.jpclett.0c00874
J. Phys. Chem. Lett. 2020, 11, 3821−3827

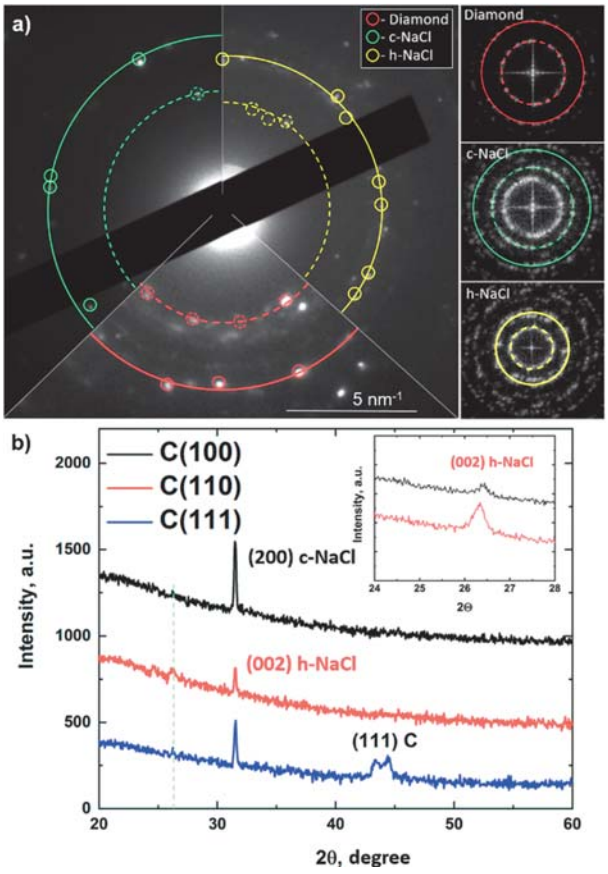

Figure 4. (a) Experimental SAED image with marked reflections that correspond to diamond (red circles), cubic NaCl (green circles), and h-NaCl (yellow circles). For calculations the average diamond grain size was 51 nm. Dashed and solid circles correspond to dashed and solid reflection marks. (b) X-ray diffraction pattern of deposited thin NaCl film on (100), (111), and (110) diamond surfaces. The most intense peak of (002) h-NaCl was observed for (110) diamond.

2θ (see Figure 4b). The average thickness of observed h-NaCl is around 6 nm. As the thickness of the NaCl film increases, the hexagonal (stable for NaCl surface) converts to cubic structure, which is known to be the most durable in the bulk.

The enlargement of the XRD diffraction pattern (see Figure 4b) shows in detail and without any doubt the presence of the (002) peak which corresponds to the presence of a new h-NaCl structure on the (110) diamond substrate (with respect to the noise from the low-intensity peak for (100) diamond). The obtained results show the influence of the substrate on the physical and even structural properties of formed 2D material and completely confirm the theoretical predictions of the evolutionary algorithm USPEX of this exotic 2D crystal structure.

We showed that NaCl possesses strong binding with the diamond (110) substrate allowing the formation of hexagonal NaCl layers on the diamond. The strong binding with diamond and the wide electronic band gap of ~6.5 eV[2] makes this material promising for applications in diamond FETs as gate dielectric instead of h-BN (as h-BN has a weak binding with diamond and lower band gap ~6 eV[64]).

In conclusion, state-of-the-art theoretical techniques of global optimizations allowed us to predict the existence of a new h-NaCl ultrathin film on the diamond (110) substrate. The strong binding stabilizes this unusual NaCl structure with the substrate, which cannot be observed on metallic substrates. Performed experimental synthesis of h-NaCl film and its characterization by SAED and XRD methods confirm our theoretical predictions entirely. We experimentally observed the formation of the exotic h-NaCl thin film on the (110) diamond substrate and distorted cubic NaCl thin film on the (100) diamond substrate. The obtained results show that reduced dimensionality can lead to exotic structures, and strong binding to substrate stabilizes two-dimensional phases—among which many are structurally and chemically very unusual, even for such seemingly simple systems as NaCl. This work is yet another proof of the reliability of the evolutionary algorithm USPEX for structure prediction, which is a powerful tool for predicting novel structures.

■ ASSOCIATED CONTENT

Supporting Information

The Supporting Information is available free of charge at https://pubs.acs.org/doi/10.1021/acs.jpclett.0c00874.

Detailed description of computational methodology; data on the simulations of the formation of NaCl films on the metal substrates, electron localization functions of predicted structure on diamond substrates, and simulations of SAED; details of experimental synthesis of NaCl on diamond substrates as well as description of X-ray scattering and SAED measurements (PDF)

■ AUTHOR INFORMATION

Corresponding Authors

Stanislav A. Evlashin − *Skolkovo Institute of Science and Technology, Moscow 121205, Russia;* orcid.org/0000-0001-6565-3748; Email: S.Evlashin@skoltech.ru

Alexander G. Kvashnin − *Skolkovo Institute of Science and Technology, Moscow 121205, Russia;* orcid.org/0000-0002-0718-6691; Email: A.Kvashnin@skoltech.ru

Authors

Kseniya A. Tikhomirova − *Skolkovo Institute of Science and Technology, Moscow 121205, Russia*

Christian Tantardini − *Skolkovo Institute of Science and Technology, Moscow 121205, Russia;* orcid.org/0000-0002-2412-9859

Ekaterina V. Sukhanova − *Emanuel Institute of Biochemical Physics RAS, Moscow 119334, Russia; Moscow Institute of Physics and Technology, Dolgoprudny 141700, Russia;* orcid.org/0000-0002-3544-2365

Zakhar I. Popov − *Emanuel Institute of Biochemical Physics RAS, Moscow 119334, Russia*

Mikhail A. Tarkhov − *Institute of Nanotechnologies of Microelectronics of the Russian Academy of Sciences, Moscow 119991, Russia*

Vladislav L. Zhdanov − *Higher School of Economics, Moscow 101000, Russia*

Alexander A. Dudin − *Institute of Nanotechnologies of Microelectronics of the Russian Academy of Sciences, Moscow 119991, Russia*

Artem R. Oganov − *Skolkovo Institute of Science and Technology, Moscow 121205, Russia; Moscow Institute of Physics and Technology, Dolgoprudny 141700, Russia; International Center for Materials Discovery, Northwestern*

https://dx.doi.org/10.1021/acs.jpclett.0c00874
J. Phys. Chem. Lett. 2020, 11, 3821−3827

Polytechnical University, Xi'an 710072, China; orcid.org/0000-0001-7082-9728

Dmitry G. Kvashnin − *Emanuel Institute of Biochemical Physics RAS, Moscow 119334, Russia; Moscow Institute of Physics and Technology, Dolgoprudny 141700, Russia;* orcid.org/0000-0003-3320-6657

Complete contact information is available at: https://pubs.acs.org/10.1021/acs.jpclett.0c00874

Notes

The authors declare no competing financial interest.

■ ACKNOWLEDGMENTS

The authors thank Dr. Victor P. Martovitsky for XRD measurements. Dr. D.-M. Tang and Dr. K.L. Firestein for help in a discussion of diffraction patterns. Z.I.P., E.V.S, K.A.T., and D.G.K. acknowledge financial support from Russian Science Foundation (No. 18-73-10135) for calculation of the formation process of NaCl thin films on metallic and diamond substrates, SAED calculation, and analysis of diffraction patterns. C.T., A.R.O, and A.G.K. acknowledge financial support from Russian Science Foundation (No. 19-72-30043) for the binding energy calculations and XRD interpretation. Calculations were performed on Rurik supercomputer at MIPT and Arkuda supercomputer of Skolkovo Foundation. We also thank Joint Supercomputer Center of the Russian Academy of Sciences for generous grants of computer time.

■ REFERENCES

(1) Sasama, Y.; Komatsu, K.; Moriyama, S.; Imura, M.; Teraji, T.; Watanabe, K.; Taniguchi, T.; Uchihashi, T.; Takahide, Y. High-Mobility Diamond Field Effect Transistor with a Monocrystalline h-BN Gate Dielectric. *APL Mater.* **2018**, *6* (11), 111105.

(2) Luo, B.; Yao, Y.; Tian, E.; Song, H.; Wang, X.; Li, G.; Xi, K.; Li, B.; Song, H.; Li, L. Graphene-like Monolayer Monoxides and Monochlorides. *Proc. Natl. Acad. Sci. U. S. A.* **2019**, *116* (35), 17213−17218.

(3) Sone, J.; Yamagami, T.; Aoki, Y.; Nakatsuji, K.; Hirayama, H. Epitaxial Growth of Silicene on Ultra-Thin Ag(111) Films. *New J. Phys.* **2014**, *16* (9), 095004.

(4) Lalmi, B.; Oughaddou, H.; Enriquez, H.; Kara, A.; Vizzini, S.; Ealet, B.; Aufray, B. Epitaxial Growth of a Silicene Sheet. *Appl. Phys. Lett.* **2010**, *97*, 223109.

(5) Saxena, S.; Chaudhary, R. P.; Shukla, S. Stanene: Atomically Thick Free-Standing Layer of 2D Hexagonal Tin. *Sci. Rep.* **2016**, *6* (1), 31073.

(6) Mannix, A. J.; Zhou, X.-F.; Kiraly, B.; Wood, J. D.; Alducin, D.; Myers, B. D.; Liu, X.; Fisher, B. L.; Santiago, U.; Guest, J. R.; Yacaman, M. J.; Ponce, A.; Oganov, A. R.; Hersam, M. C.; Guisinger, N. P. Synthesis of Borophenes: Anisotropic, Two-Dimensional Boron Polymorphs. *Science* **2015**, *350* (6267), 1513−1516.

(7) Kano, E.; Kvashnin, D. G.; Sakai, S.; Chernozatonskii, L. A.; Sorokin, P. B.; Hashimoto, A.; Takeguchi, M. One-Atom-Thick 2D Copper Oxide Clusters on Graphene. *Nanoscale* **2017**, *9* (11), 3980−3985.

(8) Zhao, J.; Deng, Q.; Bachmatiuk, A.; Sandeep, G.; Popov, A.; Eckert, J.; Rümmeli, M. H. Free-Standing Single-Atom-Thick Iron Membranes Suspended in Graphene Pores. *Science* **2014**, *343* (6176), 1228−1232.

(9) Larionov, K. V.; Kvashnin, D. G.; Sorokin, P. B. 2D FeO: A New Member in 2D Metal Oxide Family. *J. Phys. Chem. C* **2018**, *122* (30), 17389−17394.

(10) Larionov, K. V.; Popov, Z. I.; Vysotin, M. A.; Kvashnin, D. G.; Sorokin, P. B. Study of the New Two-Dimensional Compound CoC. *JETP Lett.* **2018**, *108* (1), 13−17.

(11) Yue, C.; Weng, X.-J.; Gao, G.; Oganov, A. R.; Dong, X.; Shao, X.; Wang, X.; Sun, J.; Xu, B.; Wang, H.-T.; Zhou, X.-F.; Tian, Y. Discovery of Copper Boride on Cu(111). *ArXiv*, **2019**, 1912.06027.

(12) Novoselov, K. S.; Geim, A. K.; Morozov, S. V.; Jiang, D.; Zhang, Y.; Dubonos, S. V.; Grigorieva, I. V.; Firsov, A. A. Electric Field Effect in Atomically Thin Carbon Films. *Science* **2004**, *306* (5696), 666−669.

(13) Gao, L.; Guest, J. R.; Guisinger, N. P. Epitaxial Graphene on Cu(111). *Nano Lett.* **2010**, *10* (9), 3512−3516.

(14) Suntola, T. Atomic Layer Epitaxy. *Mater. Sci. Rep.* **1989**, *4* (5), 261−312.

(15) Roth, S.; Matsui, F.; Greber, T.; Osterwalder, J. Chemical Vapor Deposition and Characterization of Aligned and Incommensurate Graphene/Hexagonal Boron Nitride Heterostack on Cu(111). *Nano Lett.* **2013**, *13* (6), 2668−2675.

(16) Shi, Y.; Zhou, W.; Lu, A.-Y.; Fang, W.; Lee, Y.-H.; Hsu, A. L.; Kim, S. M.; Kim, K. K.; Yang, H. Y.; Li, L.-J.; Idrobo, J.-C.; Kong, J. Van Der Waals Epitaxy of MoS2 Layers Using Graphene As Growth Templates. *Nano Lett.* **2012**, *12* (6), 2784−2791.

(17) Vinogradov, N. A.; Zakharov, A. A.; Ng, M. L.; Mikkelsen, A.; Lundgren, E.; Mårtensson, N.; Preobrajenski, A. B. One-Dimensional Corrugation of the h-BN Monolayer on Fe(110). *Langmuir* **2012**, *28* (3), 1775−1781.

(18) Nagashima, A.; Tejima, N.; Gamou, Y.; Kawai, T.; Oshima, C. Electronic Dispersion Relations of Monolayer Hexagonal Boron Nitride Formed on the Ni(111) Surface. *Phys. Rev. B: Condens. Matter Mater. Phys.* **1995**, *51* (7), 4606−4613.

(19) Preobrajenski, A. B.; Ng, M. L.; Vinogradov, N. A.; Vinogradov, A. S.; Lundgren, E.; Mikkelsen, A.; Mårtensson, N. Impact of Oxygen Coadsorption on Intercalation of Cobalt under the H-BN Nanomesh. *Nano Lett.* **2009**, *9* (7), 2780−2787.

(20) Suemitsu, M.; Filimonov, S. N. 3 - Understanding Crystal Growth Mechanisms in Silicon−Germanium (SiGe) Nanostructures. In *Silicon−Germanium (SiGe) Nanostructures*; Shiraki, Y., Usami, N., Eds.; Woodhead Publishing Series in Electronic and Optical Materials; Woodhead Publishing, 2011; pp 45−71.

(21) Jiang, W.; Yin, L.; Chen, H.; Paschall, A. V.; Zhang, L.; Fu, W.; Zhang, W.; Todd, T.; Yu, K. S.; Zhou, S.; Zhen, Z.; Butler, M.; Yao, L.; Zhang, F.; Shen, Y.; Li, Z.; Yin, A.; Yin, H.; Wang, X.; Avci, F. Y.; Yu, X.; Xie, J. NaCl Nanoparticles as a Cancer Therapeutic. *Adv. Mater.* **2019**, *31* (46), 1904058.

(22) Fernández-López, J.; Sayas-Barberá, E.; Pérez-Alvarez, J. A.; Aranda-Catalá, V. Effect of Sodium Chloride, Sodium Tripolyphosphate and PH on Color Properties of Pork Meat. *Color Res. Appl.* **2004**, *29* (1), 67−74.

(23) Chen, X.; Ma, Y. High-Pressure Structures and Metallization of Sodium Chloride. *EPL Europhys. Lett.* **2012**, *100* (2), 26005 (4).

(24) Tasker, P. W. The Surface Energies, Surface Tensions and Surface Structure of the Alkali Halide Crystals. *Philos. Mag. A* **1979**, *39*, 119−136.

(25) *Surface Science: Foundations of Catalysis and Nanoscience*, 3rd ed.; Kolasinski, K. W., Ed.; Wiley, 2002.

(26) Riemann, A.; Fölsch, S.; Rieder, K. H. Epitaxial Growth of Alkali Halides on Stepped Metal Surfaces. *Phys. Rev. B: Condens. Matter Mater. Phys.* **2005**, *72* (12), 125423.

(27) Guo, Q.; Qin, Z.; Liu, C.; Zang, K.; Yu, Y.; Cao, G. Bias Dependence of Apparent Layer Thickness and Moiré Pattern on NaCl/Cu(001). *Surf. Sci.* **2010**, *604* (19), 1820−1824.

(28) Wagner, M.; Negreiros, F. R.; Sementa, L.; Barcaro, G.; Surnev, S.; Fortunelli, A.; Netzer, F. P. Nanostripe Pattern of NaCl Layers on Cu(110). *Phys. Rev. Lett.* **2013**, *110* (21), 216101.

(29) Bennewitz, R.; Bammerlin, M.; Guggisberg, M.; Loppacher, C.; Baratoff, A.; Meyer, E.; Güntherodt, H.-J. Aspects of Dynamic Force Microscopy on NaCl/Cu(111): Resolution, Tip−Sample Interactions and Cantilever Oscillation Characteristics. *Surf. Interface Anal.* **1999**, *27* (5−6), 462−466.

(30) Bennewitz, R.; Foster, A. S.; Kantorovich, L. N.; Bammerlin, M.; Loppacher, Ch.; Schär, S.; Guggisberg, M.; Meyer, E.; Shluger, A. L. Atomically Resolved Edges and Kinks of NaCl Islands on Cu(111): Experiment and Theory. *Phys. Rev. B: Condens. Matter Mater. Phys.* **2000**, *62* (3), 2074−2084.
(31) Repp, J.; Meyer, G.; Paavilainen, S.; Olsson, F. E.; Persson, M. Scanning Tunneling Spectroscopy of Cl Vacancies in NaCl Films: Strong Electron-Phonon Coupling in Double-Barrier Tunneling Junctions. *Phys. Rev. Lett.* **2005**, *95* (22), 225503.
(32) Mishima, R.; Takada, M.; Tada, H. STM Studies of NaCl Thin Films on Cu(111) Surface at Low Temperature. *Mol. Cryst. Liq. Cryst.* **2007**, *472* (1), 321−325.
(33) Li, Y. J.; Kinoshita, Y.; Tenjin, K.; Ma, Z. M.; Kou, L. L.; Naitoh, Y.; Kageshima, M.; Sugawara, Y. Force Mapping of the NaCl(100)/Cu(111) Surface by Atomic Force Microscopy at 78 K. *Jpn. J. Appl. Phys.* **2012**, *51* (3R), 035201.
(34) Kakudate, T.; Nakaya, M.; Nakayama, T. Local Modification of NaCl Thin Films on Cu(111) under Different Bias Voltages. *Thin Solid Films* **2012**, *520* (6), 2004−2008.
(35) Gerß, B.; Osterloh, N.; Heidorn, S.-C.; Morgenstern, K. Diffusion Limited Aggregation in Low Temperature Growth of Sodium Chloride. *Cryst. Growth Des.* **2015**, *15* (6), 3046−3051.
(36) Fölsch, S.; Helms, A.; Zöphel, S.; Repp, J.; Meyer, G.; Rieder, K. H. Self-Organized Patterning of an Insulator-on-Metal System by Surface Faceting and Selective Growth: NaCl/Cu(211). *Phys. Rev. Lett.* **2000**, *84* (1), 123−126.
(37) Pivetta, M.; Patthey, F.; Stengel, M.; Baldereschi, A.; Schneider, W.-D. Local Work Function Moir\'e Pattern on Ultrathin Ionic Films: NaCl on Ag(100). *Phys. Rev. B: Condens. Matter Mater. Phys.* **2005**, *72* (11), 115404.
(38) Matthaei, F.; Heidorn, S.; Boom, K.; Bertram, C.; Safiei, A.; Henzl, J.; Morgenstern, K. Coulomb Attraction during the Carpet Growth Mode of NaCl. *J. Phys.: Condens. Matter* **2012**, *24* (35), 354006.
(39) Cabailh, G.; Henry, C. R.; Barth, C. Thin NaCl Films on Silver (001): Island Growth and Work Function. *New J. Phys.* **2012**, *14* (10), 103037.
(40) Heidorn, S.; Bertram, C.; Koch, J.; Boom, K.; Matthaei, F.; Safiei, A.; Henzl, J.; Morgenstern, K. Influence of Substrate Surface-Induced Defects on the Interface State between NaCl(100) and Ag(111). *J. Phys. Chem. C* **2013**, *117* (31), 16095−16103.
(41) Heidorn, S.-C.; Sabellek, A.; Morgenstern, K. Size Dependence of the Dispersion Relation for the Interface State between NaCl(100) and Ag(111). *Nano Lett.* **2014**, *14* (1), 13−17.
(42) Sun, X.; Felicissimo, M. P.; Rudolf, P.; Silly, F. NaCl Multi-Layer Islands Grown on Au(111)-(22\times \sqrt 3) Probed by Scanning Tunneling Microscopy. *Nanotechnology* **2008**, *19* (49), 495307.
(43) Shi, G.; Chen, L.; Yang, Y.; Li, D.; Qian, Z.; Liang, S.; Yan, L.; Li, L. H.; Wu, M.; Fang, H. Two-Dimensional Na−Cl Crystals of Unconventional Stoichiometries on Graphene Surface from Dilute Solution at Ambient Conditions. *Nat. Chem.* **2018**, *10* (7), 776−779.
(44) Kvashnin, A. G.; Kvashnin, D. G.; Oganov, A. R. Novel Unexpected Reconstructions of (100) and (111) Surfaces of NaCl: Theoretical Prediction. *Sci. Rep.* **2019**, *9* (1), 14267.
(45) Kvashnin, A. G.; Sorokin, P. B.; Tománek, D. Graphitic Phase of NaCl. Bulk Properties and Nanoscale Stability. *J. Phys. Chem. Lett.* **2014**, *5* (22), 4014−4019.
(46) Sorokin, P. B.; Kvashnin, A. G.; Zhu, Z.; Tománek, D. Spontaneous Graphitization of Ultrathin Cubic Structures: A Computational Study. *Nano Lett.* **2014**, *14* (12), 7126−7130.
(47) Kvashnin, A. G.; Pashkin, E. Y.; Yakobson, B. I.; Sorokin, P. B. Ionic Graphitization of Ultrathin Films of Ionic Compounds. *J. Phys. Chem. Lett.* **2016**, *7*, 2659−2663.
(48) Oganov, A. R.; Glass, C. W. Crystal Structure Prediction Using Ab Initio Evolutionary Techniques: Principles and Applications. *J. Chem. Phys.* **2006**, *124*, 244704.
(49) Zhu, Q.; Li, L.; Oganov, A. R.; Allen, P. B. Evolutionary Method for Predicting Surface Reconstructions with Variable Stoichiometry. *Phys. Rev. B: Condens. Matter Mater. Phys.* **2013**, *87* (19), 195317.
(50) Lyakhov, A. O.; Oganov, A. R.; Stokes, H. T.; Zhu, Q. New Developments in Evolutionary Structure Prediction Algorithm USPEX. *Comput. Phys. Commun.* **2013**, *184*, 1172−1182.
(51) Kresse, G.; Hafner, J. Ab Initio Molecular Dynamics for Liquid Metals. *Phys. Rev. B: Condens. Matter Mater. Phys.* **1993**, *47*, 558−561.
(52) Kresse, G.; Furthmüller, J. Efficiency of Ab-Initio Total Energy Calculations for Metals and Semiconductors Using a Plane-Wave Basis Set. *Comput. Mater. Sci.* **1996**, *6*, 15−50.
(53) Kresse, G.; Furthmüller, J. Efficient Iterative Schemes for Ab Initio Total-Energy Calculations Using a Plane-Wave Basis Set. *Phys. Rev. B: Condens. Matter Mater. Phys.* **1996**, *54*, 11169−11186.
(54) Kresse, G.; Joubert, D. From Ultrasoft Pseudopotentials to the Projector Augmented-Wave Method. *Phys. Rev. B: Condens. Matter Mater. Phys.* **1999**, *59* (3), 1758−1775.
(55) Dion, M.; Rydberg, H.; Schröder, E.; Langreth, D. C.; Lundqvist, B. I. Van Der Waals Density Functional for General Geometries. *Phys. Rev. Lett.* **2004**, *92* (24), 246401.
(56) Savin, A.; Nesper, R.; Wengert, S.; Fässler, T. F. ELF: The Electron Localization Function. *Angew. Chem., Int. Ed. Engl.* **1997**, *36* (17), 1808−1832.
(57) Johnson, E. R.; Keinan, S.; Mori-Sánchez, P.; Contreras-García, J.; Cohen, A. J.; Yang, W. Revealing Noncovalent Interactions. *J. Am. Chem. Soc.* **2010**, *132* (18), 6498−6506.
(58) Otero-De-La-Roza, A.; Johnson, E. R.; Contreras-García, J. Revealing Non-Covalent Interactions in Solids: NCI Plots Revisited. *Phys. Chem. Chem. Phys.* **2012**, *14* (35), 12165−12172.
(59) Saleh, G.; Gatti, C.; Lo Presti, L.; Contreras-García, J. Revealing Non-Covalent Interactions in Molecular Crystals through Their Experimental Electron Densities. *Chem. - Eur. J.* **2012**, *18* (48), 15523−15536.
(60) Contreras-García, J.; Johnson, E. R.; Keinan, S.; Chaudret, R.; Piquemal, J.-P.; Beratan, D. N.; Yang, W. NCIPLOT: A Program for Plotting Noncovalent Interaction Regions. *J. Chem. Theory Comput.* **2011**, *7* (3), 625−632.
(61) Otero-De-La-Roza, A.; Blanco, M. A.; Pendás, A. M.; Luaña, V. Critic: A New Program for the Topological Analysis of Solid-State Electron Densities. *Comput. Phys. Commun.* **2009**, *180* (1), 157−166.
(62) Otero-De-La-Roza, A.; Johnson, E. R.; Luaña, V. Critic2: A Program for Real-Space Analysis of Quantum Chemical Interactions in Solids. *Comput. Phys. Commun.* **2014**, *185* (3), 1007−1018.
(63) Coleman, J. N.; Lotya, M.; O'Neill, A.; Bergin, S. D.; King, P. J.; Khan, U.; Young, K.; Gaucher, A.; De, S.; Smith, R. J.; Shvets, I. V.; Arora, S. K.; Stanton, G.; Kim, H.-Y.; Lee, K.; Kim, G. T.; Duesberg, G. S.; Hallam, T.; Boland, J. J.; Wang, J. J.; Donegan, J. F.; Grunlan, J. C.; Moriarty, G.; Shmeliov, A.; Nicholls, R. J.; Perkins, J. M.; Grieveson, E. M.; Theuwissen, K.; McComb, D. W.; Nellist, P. D.; Nicolosi, V. Two-Dimensional Nanosheets Produced by Liquid Exfoliation of Layered Materials. *Science* **2011**, *331* (6017), 568−571.
(64) Zhang, K.; Feng, Y.; Wang, F.; Yang, Z.; Wang, J. Two Dimensional Hexagonal Boron Nitride (2D-HBN): Synthesis, Properties and Applications. *J. Mater. Chem. C* **2017**, *5* (46), 11992−12022.

https://dx.doi.org/10.1021/acs.jpclett.0c00874
J. Phys. Chem. Lett. 2020, 11, 3821−3827